

# Evaluation of aluminosilicate glass sintering during differential scanning calorimetry

J.P. Souza<sup>1</sup>, J.R. Martinelli<sup>1</sup>

*Nuclear and Energy Research Institute, Sao Paulo, SP, Brazil*

Received 14 August 2014; received in revised form 19 November 2014; accepted 4 February 2015

Available online 13 February 2015

## Abstract

The aim of this work is to investigate a difference in heat flow observed in the differential scanning calorimetry curves when aluminosilicate glasses are analyzed. Glasses with nominal composition 56.21 SiO<sub>2</sub> 18.65 Al<sub>2</sub>O<sub>3</sub> 25.14 MgO (wt%) were produced by the conventional melting process. Glass frits were milled and sieved in the range of 45–63 μm. The material was analyzed by X-ray fluorescence spectrometry, X-ray diffraction, differential scanning calorimetry (DSC), and differential thermal analyses (DTA). The particle size distribution was determined by laser diffraction technique. The microstructures of the samples were observed by scanning electron microscopy after removing them from the DSC sample holder. The density was determined by He pycnometry. The difference in heat flow in the DSC curves is assigned to the sintering process occurring during the heating cycle, which was confirmed by the neck formation in the particle interface, DSC signal variation in isothermal measurements, no change in the heat flow when monolith specimen are analyzed, and in subsequent DSC analysis after cooling. The concurrent crystallization was also determined.

© 2015 Elsevier Ltd and Techna Group S.r.l. All rights reserved.

*Keywords:* A. Sintering; D. Glass; Differential scanning calorimetry

## 1. Introduction

In a previous work [1], a difference in the heat flow was observed in a DSC curve when an aluminosilicate glass was investigated. At that time, no reasonable explanation was given to justify such event since on a typical DSC curve for a glass, an endothermic event assigned to the glass transition followed by an exothermic peak related to the crystallization process is generally observed [2–4]. Concerning the unexpected change in the baseline, scanning electron microscopy images showed the neck formation in the interface of particles indicating that the sintering process is occurring during the heating cycle [1,5].

The simplest case of single-phase sintering occurs when an aggregate of glass particles is heated [6]. This process is known as viscous sintering. At an initial state the material shrinks, the density

increases, and the amount of pores decreases depending on the particle size distribution, surface energy, and the viscosity of the glass phase. As the particles begin to coalesce, a viscous flow of the material towards the interparticle region originates a neck shape [6].

The most conventional techniques to study the sintering process are related to the determination of the material shrinkage. The microstructural features can also provide information about the sintering process. The initial shrinkage of the viscous flow sintering process is predicted by the Frenkel model, and for higher densities, when the pores are isolated in the matrix, the Mackenzie–Shuttleworth model is usually adopted. Both models show that the density variation depends on the temperature-dependent shear viscosity, the glass–vapor surface energy, and the time [7].

Sintering processes are studied with DSC technique when particles are nanometric and the energy release is measured, generating an exothermic peak in the DSC analyses [8].

In the current work, it is shown that the unexpected difference in the heat flow observed in DSC curves during the heating of aluminosilicate glass powders is related to the sintering process.

*E-mail addresses:* [jpsouza@ipen.br](mailto:jpsouza@ipen.br) (J.P. Souza),

[jroberto@ipen.br](mailto:jroberto@ipen.br) (J.R. Martinelli).

<sup>1</sup>Av. Prof. Lineu Prestes, 2242, Cidade Universitaria, 05508-000 Sao Paulo, SP, Brazil.

## 2. Material and methods

### 2.1. Glass powder synthesis

The nominal composition of the glasses was established based on previously reported data [1]: 56.21 SiO<sub>2</sub>, 18.65 Al<sub>2</sub>O<sub>3</sub> and 25.14 MgO (wt%). Glasses were obtained by mixing and homogenizing Al<sub>2</sub>O<sub>3</sub>, SiO<sub>2</sub>, and MgO (analytical grade). The mixture was heated at 10 °C/min to 1550 °C and melted in an alumina crucible [1]. The liquid was kept at this temperature for 30 min and then poured into distilled water to obtain frits or in a stainless steel mold to obtain a glass piece.

The frits were crushed in a stainless steel device, milled in a planetary mill (Fritsch, model pulverizette) for 10 min, and sieved in the range of 45–63 μm for 1 h.

### 2.2. Powder characterization

The glass powder was analyzed by energy dispersion X-ray fluorescence spectrometry (Shimadzu, model EDX-720) to determine the final composition. Laser diffraction (Cilas, model 1600) was used to determine the particle size distribution, and X-ray diffraction (CuKα radiation 1.54 Å, step: 2 °/min) (Rigaku, model Miniflex) to verify the presence of crystalline phases.

### 2.3. Differential scanning calorimetry analyses

The glass was analyzed by differential scanning calorimetry (Netzsch, model Pegasus 404) using a dynamic synthetic air atmosphere, heated at the rate of 10 °C/min, in an alumina sample holder, up to 1300 °C. Glass powder and a monolith piece (a piece of glass that was poured in the stainless steel mold small enough to fit the DSC sample holder) were analyzed to evaluate the calorimetric events. In each DSC analysis about 20 mg of glass powder was used. The analyses were also performed in a platinum sample holder to check the possible effects. Different atmospheres were used, and isothermal measurements were performed to check the behavior of the DSC curve.

Differential thermal analyses (DTA) were performed to help the evaluation of the difference in the heat flow. The same equipment was used, changing the assemblage from DSC to DTA.

Thermogravimetry and mass spectrometry analyses were also performed to check the mass variation and gas release during the heating (Netzsch, model STA 402-E).

### 2.4. Sample examination after the DSC analyses

After the differential scanning calorimetry analyses, the samples were removed from the sample holder and they presented a pellet shape with dimensions in the order of 4 mm in diameter. The pellets did not adhere to the sample holder and could be pulled out easily. For further studies some pellets were also produced using a vertical external tubular furnace simulating the conditions of the thermal analyses. The pellets were analyzed by X-ray diffraction, scanning electron microscopy (Hitachi, model TM3000), and He pycnometry (Micromeritics, model AccuPyc 1130).

## 3. Results and discussion

### 3.1. Powder characterization

The final composition was determined by energy dispersion X-ray fluorescence spectrometry (EDX) as 57.39 ± 0.06 SiO<sub>2</sub>, 22.27 ± 0.06 Al<sub>2</sub>O<sub>3</sub>, 19.91 ± 0.10 MgO wt%. The values of the final composition are close to the nominal ones; the difference can be attributed to the increase of the alumina content because an alumina crucible was used to melt the raw material and a decrease in the amount of MgO is due to its volatilization during heating. The following contaminants were detected at relatively low concentrations (< 1 wt%): Ca, Fe, Cu, Zr, and S.

From the particle size distribution, the average diameter was determined to be 68 μm, and the presence of particles with size in the range of 1 to 10 μm is evident, although the selection of the particles was done by sieving in the range of 45 to 63 μm. This result can be explained considering that the particles are not perfectly spherical and have an aspect ratio greater than one.

The X-ray diffraction (XRD) pattern does not show any peaks that could be related to the presence of crystalline phases; the diffraction pattern only revealed a halo which is characteristic of amorphous materials.

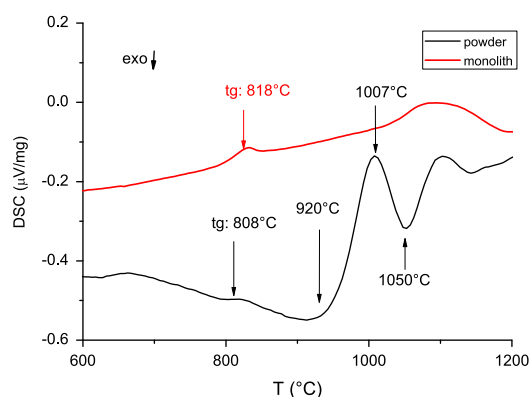


Fig. 1. DSC curves of glass samples as powder and glass monolith. The glass transition temperatures ( $T_g$ ) were determined in the range of 808–820 °C. Analyzes were performed on a dynamic synthetic air atmosphere with a heating rate of 10 °C/min in an alumina sample holder.

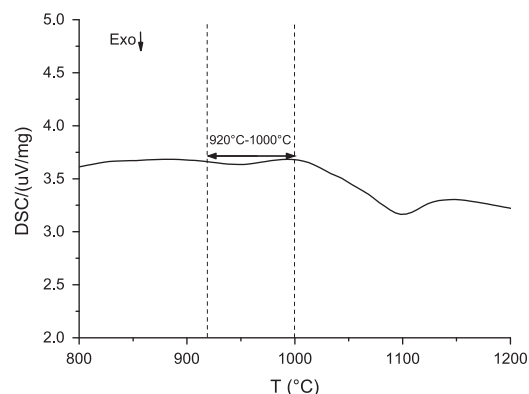


Fig. 2. DSC curve of a glass sample as powder in a platinum sample holder. The analysis was performed on a dynamic synthetic air atmosphere with a heating rate of 10 °C/min.

### 3.2. Differential scanning calorimetry analyses

Differential scanning calorimetry analyses were performed in powder and in a glass monolith. The DSC curves are shown in Fig. 1. The glass transition ( $T_g$ ) occurred in the range of 808–818 °C. The difference in the heat flow can be observed in the DSC curve of the glass powder (from 920 °C to 1007 °C), followed by an exothermic peak which can be associated to the crystallization process (maximum at 1050 °C). In the DSC curve corresponding to the glass monolith, neither the difference in the heat flow nor the crystallization peaks are observed. The crystallization phenomenon is not noticed in this curve because it mainly occurs on the surface, and the powder has a much higher specific surface area compared to the monolith glass. It is proposed that the difference in the heat flow occurring in the range of 920 °C to 1007 °C is associated with the sintering process and related to the change of the contact area between the particles and the surface of the sample holder, due to the shrinkage of the material. As evidence of this phenomenon, the difference in the heat flow is not observed in the curve of the monolithic sample, since no shrinkage takes place in the same temperature range, under the same conditions, as assumed.

The powder was analyzed in the same conditions using a platinum sample holder instead of an alumina one, and the difference in the heat flow attributed to sintering was not observed (Fig. 2), although changes in then microstructural features were observed by scanning electron microscopy (SEM) due to the sintering process. One possible explanation is that the energy transfer from the sample holder surface to the sample changes as the material shrinks during the sintering process, reducing the surface contact and generating a difference in the heat flow [5]. Since alumina has a thermal conductivity coefficient in the range of 16–31 W/m K [9] and platinum of 72 W/m K [10], the heat conduction in platinum is much faster, allowing a faster diffusion of heat throughout the sample holder. So, in this case the phenomenon is not noticed in the DSC curve.

To support the assumption that the difference in the heat flow is observed due to the surface contact between the sample holder and the sample, a differential thermal analysis (DTA) was performed following the same conditions. In the DTA the contact between the sample holder and the thermocouple is punctual, unlike in the DSC set up, where the contact occurs on the entire surface, as depicted in Fig. 3 [11]. Fig. 4 compares the curves of the DTA and DSC analyses. In the DTA there is no change in the baseline as intense as in the DSC, as expected.

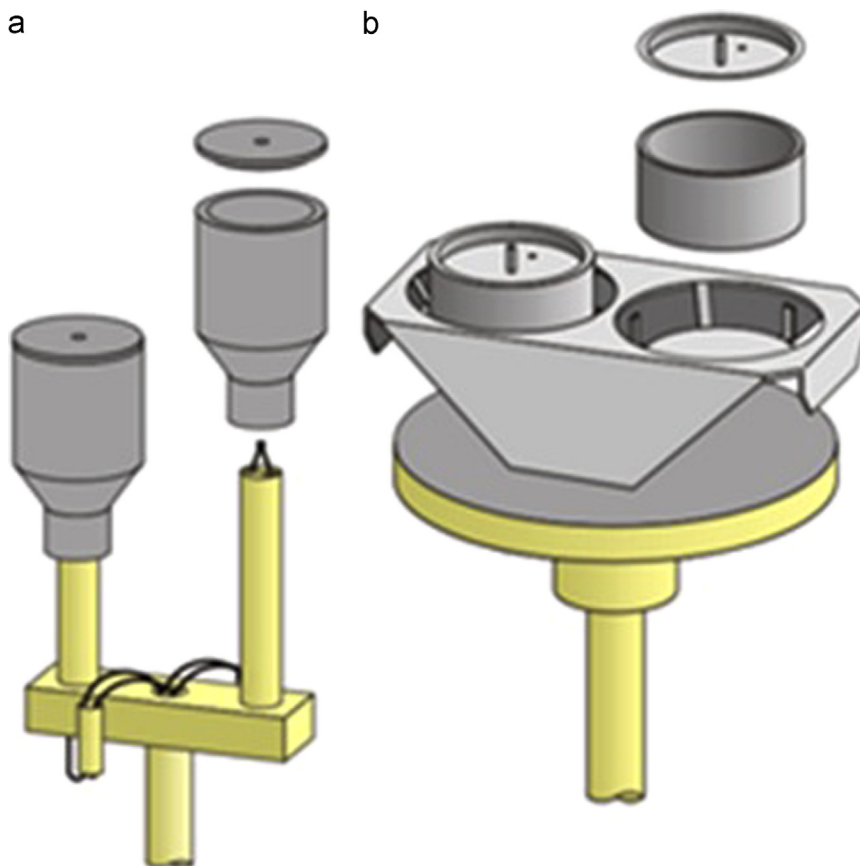


Fig. 3. Measurement assembly: (a) DTA and (b) DSC [11].

To verify the effects of the atmosphere used during the analyses, the powder was analyzed in argon and nitrogen, in addition to synthetic air (Fig. 5). The heating cycle and sample holders were the same. The endothermic and exothermic events are observed at the same temperature ranges, including the difference in the heat flow correlated to the sintering process. The atmosphere does not affect the process under investigation. Thermogravimetry and mass spectroscopy analyses were also performed in order to identify other possible effects that could justify the difference in the heat flow, but no mass change or gas release were detected.

Isothermal DSC analyses were performed at 900 °C, 920 °C, and 950 °C (Fig. 6). It was observed that the signal corresponding to the change in the heat flow is faster at higher temperatures, supporting that this event is related to the decrease of the sample surface correlated to the sintering process.

Fig. 7 shows the DSC curve of the powder initially heated to 1000 °C, where the difference in the heat flow related to sintering is noticed. Then the material was cooled down to room temperature and reheated to 1300 °C. In the following DSC curve no difference in the heat flow is present, showing that the sintering process was over. However, a crystallization peak starting at 950 °C is observed, indicating the coexistence of crystallization and sintering.

### 3.3. Pellets characterization

The micrographs of the pellets prepared in the temperature range of 940–1000 °C (Fig. 8) in an external vertical furnace show the microstructure with features corresponding to the sintering process. The formation of the neck at the interface between the particles is evident.

The densities of the pellets treated at 960 °C, 980 °C, and 1000 °C are  $2.39 \pm 0.03$ ,  $2.57 \pm 0.02$ , and  $2.54 \pm 0.05$ , respectively. The density between 960 °C and 980 °C probably increased due to the crystallization process, since the density is measured by He pycnometry.

From the results of the density study and SEM images it is possible to infer that the difference in heat flow observed in the DSC curves in the range of 920–1000 °C is associated with the process of viscous flow sintering.

In Fig. 8c and d, regions with apparent porosity are observed, indicating local absence of viscous flow sintering, due to the crystallization of the material. In these regions the material exhibits a surface crystallization inhibiting the sintering and causing the appearance of pores. The coexistence between crystallization and sintering was already pointed out in Fig. 7.

X-ray diffractions of the pellets treated at several temperatures were performed to verify the presence of crystalline phases. In Fig. 9 it is observed that only after a treatment at 980 °C, diffraction peaks related to the crystalline phases are noticeable. The identification of the phases indicates the presence of magnesium aluminum silicate, quartz and aluminum. No metallic phases were expected, although the glass contains alumina into the composition and an alumina sample holder was used to produce the pellet. Further studies are necessary.

To evaluate the densification of the material, the heat treatment was extended up to 1200 °C. However, there were no significant microstructural changes at temperatures above 1000 °C, indicating that the sintering process was over.

## 4. Conclusions

The viscous flow sintering in aluminosilicate glasses can be correlated to the difference in heat flow in the DSC curves and

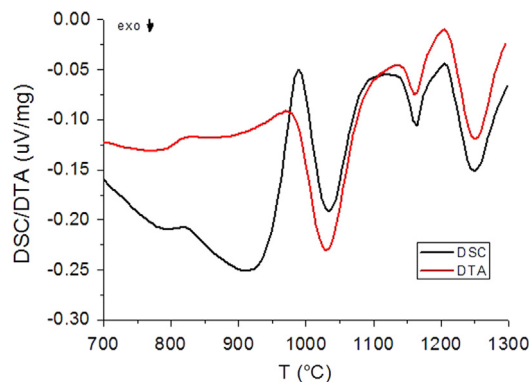


Fig. 4. DSC and DTA curves of glass powder in alumina sample holders. The analyses were performed on a dynamic synthetic air atmosphere with a heating rate of 10 °C/min.

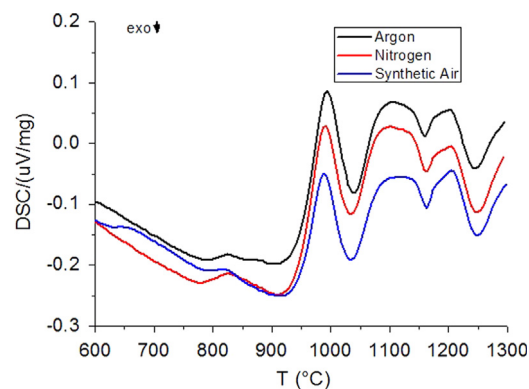


Fig. 5. DSC curves of glass powder. Analyses were performed on dynamic atmospheres of synthetic air, argon, and nitrogen. The heating rate was 10 °C/min in alumina sample holders.

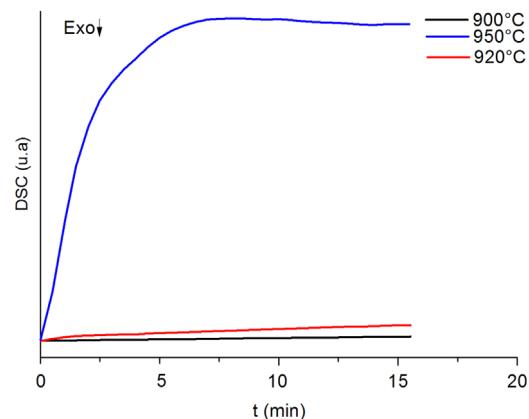


Fig. 6. Isothermal DSC curves. Analyses were performed in synthetic air atmosphere, in alumina sample holders, at 900 °C, 920 °C, and 950 °C.

confirmed by the neck formation in the particle interface, DSC signal variation in isothermal measurements, nonexistence of the difference in heat flow in monolith specimen, and in subsequent DSC analyses after cooling. The correlation of this phenomenon is only possible when the glass particles retracts during the thermal analysis and the coefficient of thermal conductivity of the sample holder is relatively low, leading to a delay in the heat transfer. Although the sintering process is an

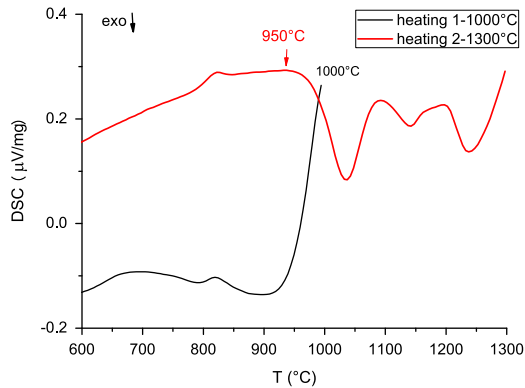


Fig. 7. DSC curves of glass powder in two steps: heated to 1000 °C, cooled to room temperature and reheated to 1300 °C. Analyses were performed on a synthetic air atmosphere, heating rate of 10 °C/min, in an alumina sample holder.

exothermic phenomenon, the event detected in DSC analysis overlaps it and is detected as a difference in heat flow.

The concurrent crystallization with the sintering process is also confirmed by the DSC analyses, the SEM micrographs and the He pycnometry data. From the DSC isotherm curves,

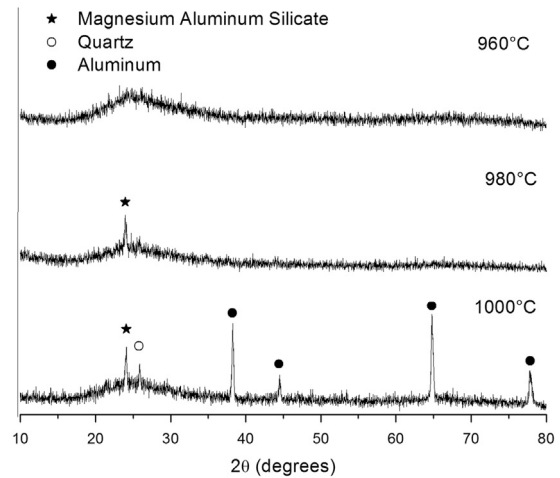


Fig. 9. X-ray diffraction patterns of pellets treated at 960 °C, 980 °C, and 1000 °C.

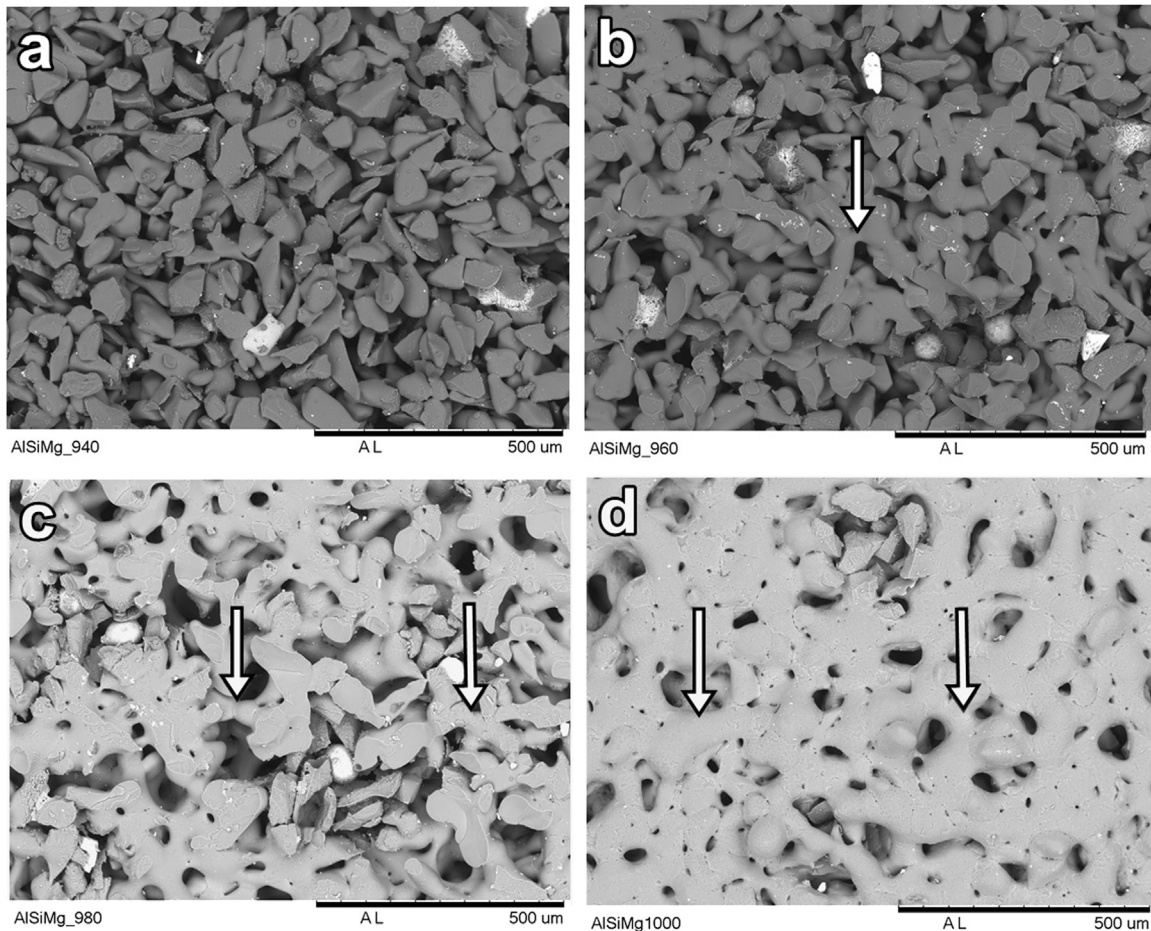


Fig. 8. SEM micrographs of the pellets treated at (a) 940 °C, (b) 960 °C, (c) 980 °C, and (d) 1000 °C. The arrows indicate the formation of necks between particles.

the DSC signal decreases at different rates demonstrating that the phenomenon depends on the temperature.

The DSC measurement was not affected by the atmosphere and no mass change or gas release was detected during the process, indicating that no endothermic event could be related to the difference in the heat flow. No other event that could be responsible for the difference in heat flow was observed. The possibility of such events is not denied, although everything indicates that the difference in heat flow is due to the DSC assemblage.

When the assembly is changed from DSC to DTA, even using an alumina sample holder, the difference in heat flow ascribed to the sintering process is not evident, confirming that the phenomenon is only noticed in the DSC analyses due to the surface heat transfer from the sample holder to the sample.

### Acknowledgements

The authors acknowledge CAPES for the scholarship granted to Juliana P. de Souza, Caroline Gugliotti for the XRD analysis, Felipe B. J. Ferrufino for the He pycnometry, Dr. Thomaz A.G. Restivo, and Dr. Douglas Gouvea for the suggestions.

### References

- [1] E.C. Barros F, F.F. Sene, J.R. Martinelli, Study of the spheronization process of glass particles for internal selective radiotherapy application, *Mater. Sci. Forum* 727–728 (2012) 1205.
- [2] N. Karpukhina, R.G. Hilla, R.V. Law, Crystallisation in oxide glasses—a tutorial review, *Chem. Soc. Rev.* 2174–2186 (2014) 43.
- [3] D. Chen, Y. Yu, P. Huang, Y. Wang, Nanocrystallization of lanthanide trifluoride in an aluminosilicate glassmatrix: dimorphism and rare earth partition, *Cryst Eng Comm* 1686–1690 (2009) 11, <http://dx.doi.org/10.1039/B904169A>.
- [4] P. Gabbott, *Principles and Applications of Thermal Analysis*, John Wiley & Sons, ISBN 0470698128, 2008, p. 418 (9780470698129).
- [5] M.W. Barsoum, *Fundamentals of Ceramics*, Institute of Physics Publishing, Bristol and Philadelphia, 2003, p. 306 (ISBN 0 7503 0902 4).
- [6] Y.M. Chiang, D. Birnie III, W.D. Kingery, *Physical Ceramics—Principles for Ceramic Science and Engineering*, Wiley—The MIT Series in Materials Science and Engineering, 1997, p. 392–398.
- [7] M.O. Prado, M.L.F. Nascimento, E.D. Zanotto, On the sinterability of crystallizing glass powders, *J. Non-Cryst. Solids* 0022-3093/354 (40–41) (2008) 4589–4597, <http://dx.doi.org/10.1016/j.jnoncrysol.2008.06.006> (<http://www.sciencedirect.com/science/article/pii/S002230930800358X>).
- [8] R.H.R. Castro, R.B. Tôrres, G.J. Pereira, D. Gouvea, Interface energy measurement of MgO and ZnO: understanding the thermodynamic stability of nanoparticles, *Chem. Mater.* 22 (2010) 2502–2509.
- [9] W.H. Gitzen, *Alumina as a Ceramic Material*, Wiley-American Ceramic Society, 1970.
- [10] *CRC Handbook of Chemistry and Physics*, in: D.R. Lide (Ed.), 84th ed., CRC Press, Boca Raton, FL, 2003.
- [11] E. Kaisersberger, From DTA to DSC and Comparison with Calculated DTA (c-DTA, SDTA) – From Measured Differential Signals to Calculated Difference Signals – NETZSCH-Gerätebau GmbH, Selb/Germany, 2005.